Atmospheric Chemistry of HFE-7200 ($C_4F_9OC_2H_5$): Reaction with OH Radicals and Fate of $C_4F_9OCH_2CH_2O(\bullet)$ and $C_4F_9OCHO(\bullet)CH_3$ Radicals

L. K. Christensen, J. Sehested, O. J. Nielsen, and M. Bilde

Atmospheric Chemistry, Building 313, Plant Biology and Biogeochemistry Department, Risø National Laboratory, DK-4000 Roskilde, Denmark

T. J. Wallington*

Ford Research Laboratory, SRL-3083, Ford Motor Company, P.O. Box 2053, Dearborn, Michigan 48121-2053

A. Guschin, L. T. Molina, and M. J. Molina

Departments of Earth, Atmospheric and Planetary Sciences and of Chemistry, Massachusetts Institute of Technology, Cambridge, Massachusetts 02139

Received: February 11, 1998; In Final Form: April 14, 1998

Relative rate techniques were used to measure $k(\mathrm{OH} + n\text{-}C_4F_9OC_2H_5) = (6.4 \pm 0.7) \times 10^{-14}$ and $k(\mathrm{OH} + i\text{-}C_4F_9OC_2H_5) = (7.7 \pm 0.8) \times 10^{-14}$ cm^3 molecule^{-1} s^{-1} at 295 K leading to estimates of ≈0.9 and 0.7 years for the atmospheric lifetimes of n-$C_4F_9OC_2H_5$ and i-$C_4F_9OC_2H_5$, respectively. A pulse radiolysis technique was used to measure $k(\mathrm{F} + \text{HFE-7200}) = (5.6 \pm 2.1) \times 10^{-11}$ cm^3 molecule^{-1} s^{-1} (HFE-7200 = $C_4F_9OC_2H_5$) at 296 K. Using FTIR−smog chamber relative rate techniques the following rate constants were determined at 296 K: $k(\mathrm{F} + \text{HFE-7200}) = (5.5 \pm 1.1) \times 10^{-11}$, $k(\mathrm{Cl} + \text{HFE-7200}) = (2.7 \pm 0.6) \times 10^{-12}$, and $k(\mathrm{Cl} + C_4F_9OC(O)CH_3) < 7 \times 10^{-13}$ cm^3 molecule^{-1} s^{-1}. Two competing loss mechanisms for $C_4F_9OCHO(\bullet)CH_3$ radicals were identified in 700 Torr of N_2/O_2 diluent at 296 K; reaction with O_2 and decomposition via C−C bond scission with $k_{O_2}/k_{decomp} = 0.026 \pm 0.010$ Torr^{-1}. The Cl atom initiated oxidation of HFE-7200 in N_2/O_2 diluent gives two products: $C_4F_9OC(O)CH_3$ and $C_4F_9OC(O)H$. $C_4F_9OC(O)CH_3$ is the major atmospheric oxidation product of HFE-7200; $C_4F_9OC(O)H$ is a minor product. The results are discussed with respect to the atmospheric chemistry of hydrofluoroethers.

1. Introduction

Recognition of the adverse effect of chlorofluorocarbon (CFC) release into the atmosphere[1,2] has led to an international effort to replace CFCs with environmentally acceptable alternatives. Hydrofluoroethers (HFEs) such as HFE-7100 ($C_4F_9OCH_3$) and HFE-7200 ($C_4F_9OC_2H_5$) are fluids designed to replace CFCs in applications such as the cleaning of electronic equipment, heat transfer agents in refrigeration systems, and carrier fluids for lubricant deposition.[3] HFE-7200 is a volatile liquid with a vapor pressure of 97 Torr at 22 °C [3] and will be released into the atmosphere during its use. Prior to its large scale industrial use an assessment of the atmospheric chemistry, and hence environmental impact, of HFE-7200 is needed.

The atmospheric oxidation of HFE-7200 will be initiated by reaction with OH radicals. The alkyl radicals produced in reaction 1 will add O_2 to give the corresponding peroxy radicals.

$$C_4F_9OCH_2CH_3 + OH \rightarrow C_4F_9OCH(\bullet)CH_3 + H_2O \quad (1a)$$

$$C_4F_9OCH_2CH_3 + OH \rightarrow C_4F_9OCH_2CH_2(\bullet) + H_2O \quad (1b)$$

$$C_4F_9OCH(\bullet)CH_3 + O_2 + M \rightarrow C_4F_9OCHOO(\bullet)CH_3 + M \quad (2a)$$

$$C_4F_9OCH_2CH_2(\bullet) + O_2 + M \rightarrow C_4F_9OCH_2CH_2OO(\bullet) + M \quad (2b)$$

$$C_4F_9OC_2H_4OO(\bullet) + NO \rightarrow C_4F_9OC_2H_4O(\bullet) + NO_2 \quad (3a)$$

$$C_4F_9OC_2H_4OO(\bullet) + NO + M \rightarrow C_4F_9OC_2H_4ONO_2 + M \quad (3b)$$

$$C_4F_9OC_2H_4OO(\bullet) + NO_2 + M \rightarrow C_4F_9OC_2H_4O_2NO_2 + M \quad (4)$$

$$C_4F_9OC_2H_4OO(\bullet) + HO_2 \rightarrow \text{products} \quad (5)$$

$$C_4F_9OC_2H_4OO(\bullet) + R'O_2 \rightarrow \text{products} \quad (6)$$

By analogy to other peroxy radicals,[4] those derived from HFE-7200 will react with NO, NO_2, HO_2, and other peroxy radicals in the atmosphere. Experiments have been performed in our laboratories to elucidate the atmospheric chemistry of HFE-7200. A relative rate approach was used at MIT to measure the kinetics of the reaction of OH radicals with HFE-7200 and hence to provide an estimate of its atmospheric lifetime. A pulse radiolysis time-resolved UV−visible spectroscopic technique was used at Risø to study the kinetics of the reaction of fluorine atoms with HFE-7200. The kinetics of the reaction of Cl and F atoms with HFE-7200 were studied at Ford using relative rate methods. Finally, the atmospheric fate of the alkoxy

* To whom correspondence should be addressed.

S1089-5639(98)01128-1 CCC: $15.00
Published on Web 05/28/1998

radicals $C_4F_9OCH_2CH_2O(\bullet)$ and $C_4F_9OCHO(\bullet)CH_3$ was studied using a FTIR spectrometer coupled to a smog chamber at Ford. The results are reported herein and discussed with respect to the environmental impact of HFE-7200 and other HFEs.

2. Experimental Section

The three experimental systems used are described in detail elsewhere.[5−7] All samples of HFE-7200 used in this work were supplied by the 3M Co. Experiments performed at Risø employed a commercial sample of HFE-7200, which was a mixture of 35% *n*-$C_4F_9OC_2H_5$ ($CF_3CF_2CF_2CF_2OC_2H_5$) and 65% *i*-$C_4F_9OC_2H_5$ ($(CF_3)_2CFCF_2OC_2H_5$). During the experiments at MIT and Ford Motor Co. a sample of pure *i*-$C_4F_9OC_2H_5$ became available and was used. In light of the structural similarities between the two HFE-7200 isomers and the rapidity of the reaction of F atoms with HFE-7200, it is assumed that the result for k(F + HFE-7200) obtained at Risø using the mixture of isomers is representative of the individual pure isomers. Evidence supporting this assumption was obtained from the work at Ford and is discussed in section 3.3. The uncertainties reported in this paper are two standard deviations unless otherwise stated. Standard error propagation methods were used to calculate combined uncertainties.

2.1. FTIR−Photolysis System at MIT. Two samples of HFE-7200 obtained from 3M were used in the present studies. One sample (referred to in this study as i-HFE-7200) was isomerically pure (>99.9%), while the other sample (referred here as n-HFE-7200) contained 95% n- and 5% i-isomers. The value for the rate of the OH + HFE-7200 reaction was obtained by monitoring rate of disappearance of HFE-7200 relative to that of a reference compound (CH_4 or CH_3Cl) in the presence of OH radicals at 295 K. The decay of the sample was measured using Fourier transform infrared spectroscopy.[5] The concentrations of HFE-7200, CH_4, or CH_3Cl were monitored by spectral subtraction. The OH radicals were generated by photolysis of ozone at 254 nm in the presence of water vapor:

$$O_3 + h\nu \rightarrow O(^1D) + O_2 \quad (7)$$

$$O(^1D) + H_2O \rightarrow 2OH \quad (8)$$

The long-path absorption cell, made of Pyrex glass, had a volume of 7.6 L and a base length of 60 cm, which was adjusted to give a total of 24 passes and an optical path of 14.4 m. The concentrations of the reactants and products were monitored with an FTIR spectrometer (Nicolet 800). The mercury photolysis lamp (Ace Hanovia 450-W medium-pressure mercury lamp) was placed inside the absorption cell, enveloped in a Vycor tube which transmits 254-nm radiation but absorbs the 185-nm Hg line; no decay of the HFE-7200 sample was observed in the absence of ozone.

The organic reactants were mixed with helium in a 3-L glass reservoir to yield mole fractions of ∼1%. Ozone was prepared by first trapping the effluent from an ozonizer in cold silica gel and then desorbing the sample into a 12-L glass reservoir and subsequently mixing with helium. The experiments were performed at room temperature in ∼200 Torr helium, in the presence of ∼1−3 Torr ozone.

2.2. Pulse Radiolysis System at Risø National Laboratory. A pulse radiolysis transient UV absorption apparatus[6] was used to measure the rate of reaction of F atoms with HFE-7200. Radicals were generated by radiolysis of gas mixtures in a 1 L stainless steel reactor by a 30 ns pulse of 2 MeV electrons from a Febetron 705B field emission accelerator. The analyzing light was provided by a pulsed Xenon arc lamp, reflected in the reaction cell by internal White type optics (total UV path length = 80 cm), dispersed using a 1 m McPherson monochromator (operated at a spectral resolution of 0.8 nm) and detected by a photomultiplier.

SF_6 was used as the diluent gas. Radiolysis of SF_6 produces fluorine atoms:

$$SF_6 + 2\ \text{MeV}\ e^- \rightarrow F + \text{products} \quad (9)$$

SF_6 was always present in great excess to minimize the relative importance of direct radiolysis of other compounds in the gas mixtures. The fluorine atom yield at full radiolysis dose and 1000 mbar SF_6 was $(3.18 \pm 0.32) \times 10^{15}$ cm^{-3} [8] (1013 mbar = 760 Torr). Reagents used were the following: 0−27 mbar O_2 (ultrahigh purity); 950−1000 mbar SF_6 (99.9%); 0−19 mbar HFE-7200 (>99%). All were used as received. The HFE-7200 sample was repeatedly degassed by freeze−pump−thaw cycles before use.

2.3. FTIR−Smog Chamber System at Ford Motor Co. All experiments were performed in a 140-L Pyrex reactor interfaced to a Mattson Sirus 100 FTIR spectrometer.[7] The reactor was surrounded by 22 fluorescent blacklamps (GE F15T8-BL), which were used to photochemically initiate the experiments. The oxidation of HFE-7200 was initiated by reaction with Cl atoms which were generated by the photolysis of molecular chlorine in O_2/N_2 diluent at 700 Torr total pressure at 296 ± 2 K:

$$Cl_2 + h\nu \rightarrow 2Cl \quad (10)$$

$$Cl + C_4F_9OC_2H_5 \rightarrow C_4F_9OC_2H_4(\bullet) + HCl \quad (11)$$

$$C_4F_9OC_2H_4(\bullet) + O_2 + M \rightarrow C_4F_9OC_2H_4O_2(\bullet) + M \quad (2)$$

The loss of HFE-7200 and the formation of products were monitored by Fourier transform infrared spectroscopy using an infrared path length of 28 m and a resolution of 0.25 cm^{-1}. Infrared spectra were derived from 32 co-added interferograms.

Two sets of experiments were performed. First, relative rate techniques were used to determine rate constants for the reactions of Cl and F atoms with HFE-7200. Second, the products of the atmospheric oxidation of HFE-7200 were investigated by irradiating HFE-7200/Cl_2/O_2/N_2 mixtures.

Initial concentrations of the gas mixtures for the relative rate experiments were 4−9 mTorr of HFE-7200, 20−32 mTorr of the reference organic, and either 0.28−0.31 Torr of Cl_2 or 0.5−1.0 Torr of F_2, in 700 Torr of air or N_2 diluent. In the study of the oxidation of HFE-7200, reaction mixtures consisted of 4.4−7.1 mTorr *i*-$C_4F_9OC_2H_5$, 51−420 mTorr Cl_2, 0−40 mTorr of NO, and 4−700 Torr O_2 with N_2 added to a total pressure of 700 Torr. The O_2/Cl_2 concentration ratio was kept larger than 100 to suppress reaction between alkyl radicals and molecular chlorine.

3. Results and Discussion

3.1. Reaction of OH with HFE-7200 Investigated at MIT. The results of the kinetic runs for n-HFE-7200 and i-HFE-7200 using CH_3Cl as reference are presented in Figure 1A,B. Linear least-squares analysis of the data gives k(n-HFE-7200)/k(CH_3Cl) = 1.77 ± 0.14 and k(i-HFE-7200)/k(CH_3Cl) = 2.13 ± 0.09. Interestingly, there appears to be a small difference in the reactivity of the two different isomers toward OH radicals with i-HFE-7200 ($(CF_3)_2CFCF_2OC_2H_5$) being approximately 20% more reactive than n-HFE-7200 ($CF_3CF_2CF_2CF_2OC_2H_5$). Using

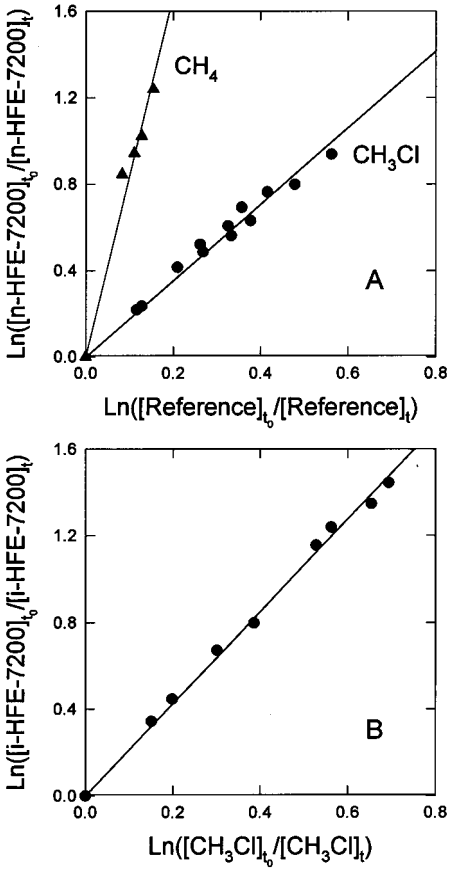

Figure 1. Decay of HFE-7200 versus CH_3Cl and CH_4 in the presence of OH radicals in 200 Torr of helium diluent at 295 K. Panel A shows data for n-HFE-7200, while panel B shows data for i-HFE-7200.

$k(CH_3Cl + OH) = 3.6 \times 10^{-14}$ cm^3 molecule^{-1} s^{-1} [9] we obtain $k(OH$ + n-HFE-7200$) = (6.4 \pm 0.7) \times 10^{-14}$ and $k(OH$ + i-HFE-7200$) = (7.7 \pm 0.8) \times 10^{-14}$ cm^3 molecule^{-1} s^{-1}. The quoted uncertainties reflect statistical uncertainties of the measurements and a 10% uncertainty in $k(CH_3Cl + OH)$.

Additional experiments were performed for n-HFE-7200 using CH_4 as reference. The results are shown in Figure 1A and give k(n-HFE-7200)/$k(CH_4) = 8.4 \pm 1.5$. Using $k(CH_4 + OH) = (6.3 \pm 0.6) \times 10^{-15}$ gives k(n-HFE-7200$) = (5.3 \pm 1.1) \times 10^{-14}$ cm^3 molecule^{-1} s^{-1}. This result is consistent with that derived from experiments using CH_3Cl as reference, but the uncertainty is much larger, since the rate of CH_4 with OH is much slower and less than 10% of the CH_4 reacted with OH. Assuming an atmospheric lifetime for methane of 9 years[10] and a rate constant for the $CH_4 + OH$ reaction of 6.3×10^{-15} cm^3 molecule^{-1} s^{-1} leads to atmospheric lifetimes against reaction with OH of ≈0.9 year for n-HFE-7200 and ≈0.7 year for i-HFE-7200.

3.2. Kinetics of the F + $C_4F_9OC_2H_5$ Reaction. The rate constant ratio k_{12}/k_{13} was determined from the maximum transient absorption at 230 nm following pulse radiolysis (32% of maximum) of mixtures of 0.3−10 mbar of HFE-7200, 50 mbar of CF_3CCl_2H, and 940−950 mbar SF_6. Reactions 12 and 13 compete for the available F atoms. The alkyl radical, CF_3-

$$F + C_4F_9OC_2H_5 \rightarrow C_4F_9OC_2H_4(\bullet) + HF \qquad (12)$$

$$F + CF_3CCl_2H \rightarrow CF_3CCl_2(\bullet) + HF \qquad (13)$$

CCl_2, formed by reaction of F atoms with CF_3CCl_2H (HCFC-123) absorbs strongly at 230 nm ($\sigma_{CF_3CCl_2} = 9.7 \times 10^{-18}$ cm^2 molecule^{-1} [11]). In contrast, absorption by the $C_4F_9OC_2H_4$ radical is significantly weaker. Figure 2 shows the observed variation of the maximum transient absorbance at 230 nm as a function of the concentration ratio [HFE-7200]/[CF_3CCl_2H]. As shown in Figure 2, the maximum transient absorption decreases with increasing HFE-7200 concentration because a greater fraction of the F atoms react with HFE-7200.

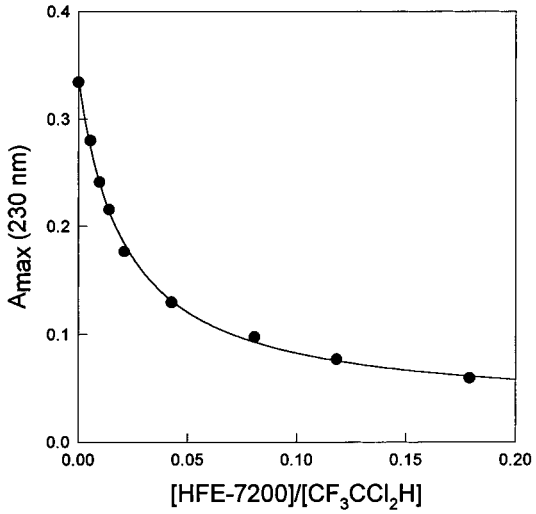

Figure 2. Maximum transient absorbance at 230 nm plotted as function of [HFE-7200]/[CF_3CCl_2H]. The smooth line is a fit to the data; see text for details.

The data in Figure 2 can be fitted with a three-parameter expression:

$$A_{max} = \frac{A_{CF_3CCl_2} + A_{C_4F_9OC_2H_4}\left[\frac{k_{12}}{k_{13}}\right]\left\{\frac{[\text{HFE-7200}]}{[CF_3CCl_2H]}\right\}}{1 + \left[\frac{k_{12}}{k_{13}}\right]\left\{\frac{[\text{HFE-7200}]}{[CF_3CCl_2H]}\right\}}$$

Here A_{max}, $A_{CF_3CCl_2}$, and $A_{C_4F_9OC_2H_4}$ are the observed maximum absorbance for the mixture of radicals, the maximum absorbance expected if all F atoms react with CF_3CCl_2H, and the maximum absorbance expected if all F atoms react with HFE-7200, respectively. $A_{CF_3CCl_2}$, $A_{C_4F_9OC_2H_4}$, and k_{12}/k_{13} were simultaneously varied, and the best fit was achieved with $A_{CF_3CCl_2} = 0.34 \pm 0.01$, $A_{C_4F_9OC_2H_4} = 0.03 \pm 0.01$, and $k_{12}/k_{13} = 47 \pm 6$. The result for $A_{CF_3CCl_2}$ is consistent with that expected on the basis of the published absorption cross section of the CF_3CCl_2 radical.[11] Using $k_{13} = (1.2 \pm 0.4) \times 10^{-12}$ [12] gives $k_{12} = (5.6 \pm 2.1) \times 10^{-11}$ cm^3 molecule^{-1} s^{-1}. This result is in good agreement with the value of $(5.5 \pm 1.1) \times 10^{-11}$ cm^3 molecule^{-1} s^{-1} determined using the FTIR technique as described in section 3.3.

3.3. Relative Rate Studies of the Reactions of Cl and F Atoms with HFE-7200. Prior to the investigation of the atmospheric oxidation products of HFE-7200, relative rate experiments were performed using the FTIR system at Ford Motor Co. to investigate the kinetics of reactions 11 and 12. The techniques used are described in detail elsewhere.[13] Photolysis of molecular halogen was used as a source of halogen atoms.

The kinetics of reaction 11 were measured relative to reactions 14−16. Reaction 12 was measured relative to reaction 17. The

$$Cl + C_2H_5Cl \rightarrow \text{products} \qquad (14)$$

$$Cl + CH_3Cl \rightarrow \text{products} \qquad (15)$$

$$Cl + CH_3OC(O)H \rightarrow \text{products} \quad (16)$$

$$F + CH_4 \rightarrow CH_3(\bullet) + HF \quad (17)$$

observed losses of HFE-7200 versus those of reference compounds in the presence of either Cl or F atoms are shown in Figures 3 and 4, respectively. All experiments described in this section, except one, were performed using a sample of HFE-7200, which consisted of 65% *i*-$C_4F_9OC_2H_5$ and 35% *n*-$C_4F_9OC_2H_5$. When a sample of pure *i*-$C_4F_9OC_2H_5$ became available, it was possible to distinguish between the IR features attributable to the two different isomers. The IR features of the i- and n-isomers decayed at the same rate showing that there is no discernible difference (<10%) in reactivity of the isomers toward F or Cl atoms. For completeness one relative rate experiment was performed using pure *i*-$C_4F_9OC_2H_5$. The result was consistent with that obtained using the mixture of isomers. Linear least-squares analysis of the data in Figures 3 and 4 gives $k_{11}/k_{14} = 0.38 \pm 0.02$, $k_{11}/k_{15} = 5.71 \pm 0.37$, $k_{11}/k_{16} = 1.70 \pm 0.06$, and $k_{12}/k_{17} = 0.81 \pm 0.04$. Using $k_{14} = 8.0 \times 10^{-12}$,[9] $k_{15} = 4.8 \times 10^{-13}$,[9] $k_{16} = 1.4 \times 10^{-12}$, and $k_{17} = 6.8 \times 10^{-11}$,[12] the four ratios give $k_{11} = (3.04 \pm 0.16) \times 10^{-12}$, $k_{11} = (2.74 \pm 0.18) \times 10^{-12}$, $k_{11} = (2.38 \pm 0.08) \times 10^{-12}$, and $k_{12} = (5.51 \pm 0.27) \times 10^{-11}$ cm^3 molecule^{-1} s^{-1}, respectively. We estimate that potential systematic errors associated with uncertainties in the reference rate constants add 10% and 20% uncertainty ranges for k_{11} and k_{12}, respectively. Propagating these additional uncertainties gives $k_{11} = (3.04 \pm 0.34) \times 10^{-12}$, $k_{11} = (2.74 \pm 0.33) \times 10^{-12}$, $k_{11} = (2.38 \pm 0.25) \times 10^{-12}$, and $k_{12} = (5.51 \pm 1.13) \times 10^{-11}$ cm^3 molecule^{-1} s^{-1}. We choose to cite a final value of k_{11} which is the average of those determined using the three different reference compounds together with error limits which encompass the extremes of the individual determinations. Hence, $k_{11} = (2.7 \pm 0.6) \times 10^{-12}$ and $k_{12} = (5.5 \pm 1.1) \times 10^{-11}$ cm^3 molecule^{-1} s^{-1}. Quoted errors reflect the accuracy of our measurements. The value of k_{12} determined using the FTIR technique is in agreement with the determination of $k_{12} = (5.6 \pm 2.1) \times 10^{-11}$ cm^3 molecule^{-1} s^{-1} obtained using the pulse radiolysis technique (see section 3.2). There are no literature data available for k_{11} or k_{12} with which to compare our results. It is interesting to note that while there is a small (≈20%) difference in the reactivity of the two HFE-7200 isomers toward OH radicals (see section 3.1), there is no discernible difference in the reactivity of the two isomers toward Cl and F atoms. This observation presumably reflects the greater reactivity (and hence low selectivity) of the reaction of Cl and F atoms with HFE-7200.

3.4. Study of the Mechanism of the Atmospheric Oxidation of $C_4F_9OC_2H_5$. The atmospheric degradation mechanism of HFE-7200 was studied using the UV irradiation of $C_4F_9OC_2H_5/Cl_2/O_2/N_2$ mixtures in the FTIR−smog chamber system at Ford Motor Co.[7] To simplify the data analysis the isomerically pure sample of 100% *i*-$C_4F_9OC_2H_5$ [$(CF_3)_2CFCF_2OC_2H_5$] was used in the product experiments. Typical spectra obtained before and after a 1 min UV irradiation of a mixture of 4.3 mTorr of *i*-$C_4F_9OCH_2CH_3$, 63 mTorr Cl_2, 52 Torr O_2, and 648 Torr of N_2 are shown in Figure 5. In all experiments perfluoroisobutyl formate, *i*-$C_4F_9OC(O)H$, was a readily observed product identified by means of its characteristic IR features at 1807 and 1822 cm^{-1}.[14] In addition to IR features attributable to i-$C_4F_9OC(O)H$ there were IR features observed at 808, 993, 1013, 1125, 1165, 1261, 1291, and 1841 cm^{-1} attributable to the formation of one (or more) unknown compound(s) which we will label "X". The increase in X scaled linearly with the loss of *i*-$C_4F_9OC_2H_5$. Experiments were performed at a constant total pressure of 700 Torr with the O_2 partial pressure varied over the range 4−700 Torr. As shown in Figure 6, as the O_2 partial pressure was increased, the yield of *i*-$C_4F_9OC(O)H$ decreased while X increased. For O_2 partial pressures greater than 300 Torr there was little change in the yields of $C_4F_9OC(O)H$ and X.

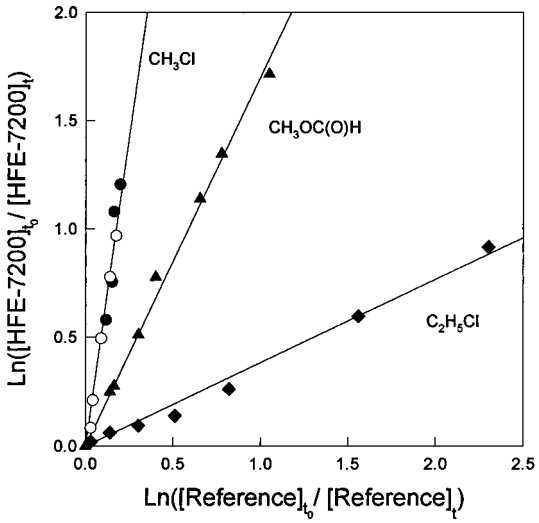

Figure 3. Decay of HFE-7200 versus C_2H_5Cl (diamonds), CH_3Cl (circles), and $CH_3OC(O)H$ (triangles) in the presence of Cl atoms. Experiments were performed at 296 K in 700 Torr of air (filled symbols) or N_2 (open symbols).

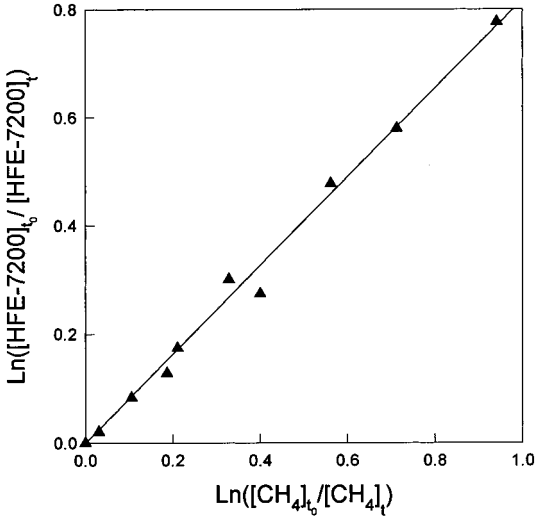

Figure 4. Decay of HFE-7200 and CH_4 in the presence of F atoms in 700 Torr of air at 296 K.

The reaction of Cl atoms with HFE-7200 in the presence of O_2 gives rise to two different peroxy radicals, which in turn will undergo self- and cross-reaction to give the corresponding alkoxy radicals:

$$i\text{-}C_4F_9OCHO_2(\bullet)CH_3 + RO_2 \rightarrow i\text{-}C_4F_9OCHO(\bullet)CH_3 + RO + O_2 \quad (18a)$$

$$i\text{-}C_4F_9OCH_2CH_2O_2(\bullet) + RO_2 \rightarrow i\text{-}C_4F_9OCH_2CH_2O(\bullet) + RO + O_2 \quad (18b)$$

There are several possible fates of these alkoxy radicals. For *i*-$C_4F_9OCHO(\bullet)CH_3$

$$i\text{-}C_4F_9OCHO(\bullet)CH_3 + M \rightarrow i\text{-}C_4F_9OC(O)H + CH_3(\bullet) + M \quad (19)$$

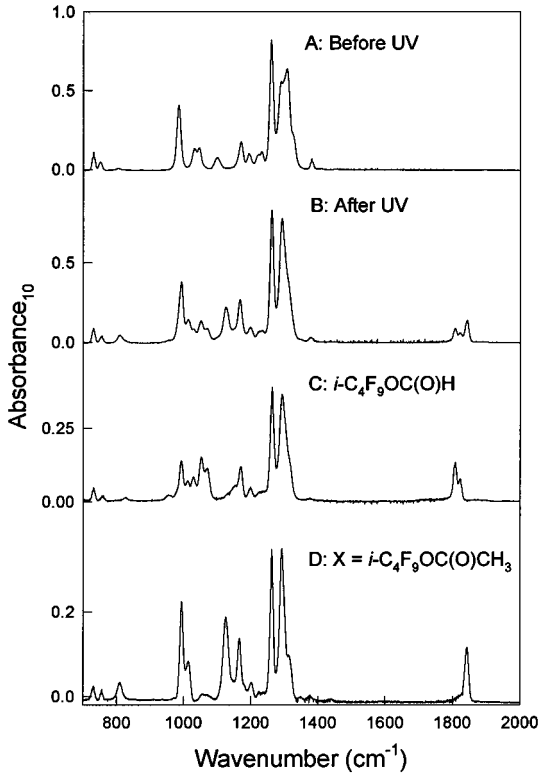

Figure 5. IR spectra before (A) and after (B) a 1 min irradiation of a mixture of 4.3 mTorr of i-HFE-7200, 63 mTorr Cl_2, 52 Torr O_2, and 648 Torr of N_2. The loss of *i*-HFE-7200 was 72%. Panel C is a reference spectrum of 1.88 mTorr of *i*-$C_4F_9OC(O)H$, and panel D is the reference spectrum of *i*-$C_4F_9OC(O)CH_3$ (1.6 mTorr).

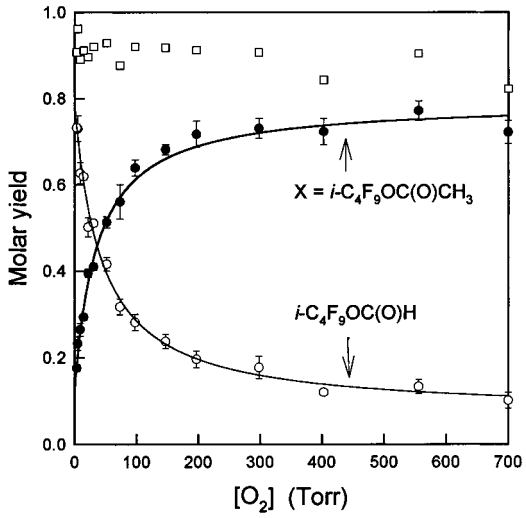

Figure 6. Observed yields of *i*-$C_4F_9OC(O)H$ (○), X ≡ *i*-$C_4F_9OC(O)CH_3$ (●), and the combined yield of these two products (□) versus the O_2 partial pressure following the UV irradiation of i-HFE-7200/Cl_2/N_2/O_2 mixtures at 700 Torr total pressure and 296 K. The curves are fits to the data; see text for details.

$$i\text{-}C_4F_9OCHO(\bullet)CH_3 + M \rightarrow i\text{-}C_4F_9OC(O)CH_3 + H(\bullet) + M \quad (20)$$

$$i\text{-}C_4F_9OCHO(\bullet)CH_3 + O_2 \rightarrow i\text{-}C_4F_9OC(O)CH_3 + HO_2(\bullet) \quad (21)$$

while for *i*-$C_4F_9OCH_2CH_2O(\bullet)$

$$i\text{-}C_4F_9OCH_2CH_2O(\bullet) + M \rightarrow i\text{-}C_4F_9OCH_2(\bullet) + HCHO + M \quad (22)$$

$$i\text{-}C_4F_9OCH_2CH_2O(\bullet) + M \rightarrow i\text{-}C_4F_9OCH_2CHO + H(\bullet) + M \quad (23)$$

$$i\text{-}C_4F_9OCH_2CH_2O(\bullet) + O_2 \rightarrow i\text{-}C_4F_9OCH_2CHO + HO_2(\bullet) \quad (24)$$

The increase in the yield of X and decrease in *i*-$C_4F_9OC(O)H$ with increasing $[O_2]$ shows that reactions 21 and/or 24 become important at high $[O_2]$. The unknown "X" is either *i*-$C_4F_9OC(O)CH_3$, *i*-$C_4F_9OCH_2CHO$, or both. There are four aspects of the IR spectrum which suggest that X is the ester *i*-$C_4F_9OC(O)CH_3$. First, the observed carbonyl stretching frequency of 1841 cm^{-1} is typical for a fluorinated ester but is ≈90 cm^{-1} higher than typically observed for an aldehyde. Second, there is no aldehydic C−H stretching feature in the 2720−2820 cm^{-1} region. Third, there is no significant $-CH_2-$ scissors feature at ≈1450 cm^{-1}. Finally, there is no −C(O)H deformation band at ≈1400 cm^{-1}. The kinetic behavior of X is also consistent with its assignment as *i*-$C_4F_9OC(O)CH_3$. Following the UV irradiation of HFE-7200/Cl_2/O_2/N_2 mixtures the IR features ascribed to X increased linearly with the loss of HFE-7200 for conversions of HFE-7200 over the range 10−85%. Evidence for loss of X via Cl attack was observed only in experiments employing >85% conversion of HFE-7200. We conclude that Cl atoms react with X at least 5 times slower than with HFE-7200; i.e., $k(Cl + X) < 7 \times 10^{-13}$ cm^3 $molecule^{-1}$ s^{-1}. All aldehydes studied to date react rapidly with Cl atoms with rate constants of typically $10^{-11}-10^{-10}$ cm^3 $molecule^{-1}$ s^{-1}.[15] In contrast, esters are relatively unreactive toward Cl atoms, for example, $k(Cl + CF_3C(O)OCH_2CF_3) = 9.4 \times 10^{-16}$ cm^3 $molecule^{-1}$ s^{-1}.[16] It seems reasonable at this point to proceed on the assumption that X is *i*-$C_4F_9OC(O)CH_3$ and that the observed dependence of the product yields on $[O_2]$ reflects a competition between reactions 19 and 21.

As shown in Figure 6, while the yield of *i*-$C_4F_9OC(O)H$ decreases as the O_2 partial pressure is increased from 3 to 300 Torr, further increase in $[O_2]$ has little or no effect and the *i*-$C_4F_9OC(O)H$ yield remains at 10−15%. This behavior suggests that there is a source of *i*-$C_4F_9OC(O)H$ which is independent of $[O_2]$. The most likely source for this *i*-$C_4F_9OC(O)H$ is the *i*-$C_4F_9OCH_2CH_2O(\bullet)$ alkoxy radical. There are three possible fates of the *i*-$C_4F_9OCH_2CH_2O(\bullet)$ radical, reactions 22−24. Decomposition via reaction 22 gives the alkyl radical *i*-$C_4F_9OCH_2(\bullet)$, which is known to react further to give *i*-$C_4F_9OC(O)H$.[14] Reactions 23 and 24 produce the aldehyde *i*-$C_4F_9OCH_2CHO$ which, as discussed above, is expected to be at least 1 order of magnitude more reactive than HFE-7200 toward Cl atoms and will be converted into *i*-$C_4F_9OCH_2(\bullet)$ radicals and hence into *i*-$C_4F_9OC(O)H$:

$$i\text{-}C_4F_9OCH_2CHO + Cl \rightarrow i\text{-}C_4F_9OCH_2C(O)(\bullet) + HCl \quad (25)$$

$$i\text{-}C_4F_9OCH_2C(O)(\bullet) + O_2 + M \rightarrow i\text{-}C_4F_9OCH_2C(O)OO(\bullet) + M \quad (26)$$

$$i\text{-}C_4F_9OCH_2C(O)OO(\bullet) + RO_2 \rightarrow i\text{-}C_4F_9OCH_2C(O)O(\bullet) + RO + O_2 \quad (27)$$

$$i\text{-}C_4F_9OCH_2C(O)O(\bullet) + M \rightarrow i\text{-}C_4F_9OCH_2(\bullet) + CO_2 + M \quad (28)$$

The decrease in the yield of *i*-$C_4F_9OC(O)H$ and increase of *i*-$C_4F_9OC(O)CH_3$ shown in Figure 6 with increasing $[O_2]$ reflects competition between reactions 19 and 21 for the available *i*-C_4F_9-

$OCHO(\bullet)CH_3$ radicals. We can place the yield of *i*-$C_4F_9OC(O)CH_3$ on an absolute basis by equating the increase in its yield to the *decrease* in the yield of *i*-$C_4F_9OC(O)H$ (for which we have an absolute calibration[14]). It was on this basis that the $C_4F_9OC(O)CH_3$ yields in Figure 6 were calibrated. As seen from Figure 6, the combined yields of *i*-$C_4F_9OC(O)H$ and *i*-$C_4F_9OC(O)CH_3$ account for ≈90% of the loss of HFE-7200. The dependence of the product yields in Figure 6 on $[O_2]$ can be used to extract a value for the rate constant ratio k_{21}/k_{19}. Assuming that the fate of *i*-$C_4F_9OCHO(\bullet)CH_3$ radicals is either decomposition via reaction 19 or reaction with O_2 and that all *i*-$C_4F_9OCH_2CH_2O(\bullet)$ radicals are converted into *i*-$C_4F_9OC(O)H$, then the yield of *i*-$C_4F_9OC(O)H$ can be related to the molar yields of the two alkoxy radicals and the rate constant ratio k_{21}/k_{19}

$$Y(C_4F_9OC(O)H) = Y(C_4F_9OCHO(\bullet)CH_3)\left[\frac{1}{\frac{k_{21}}{k_{19}}[O_2] + 1}\right] + Y(C_4F_9OCH_2CH_2O(\bullet)) \quad \text{(I)}$$

while the yield of *i*-$C_4F_9OC(O)CH_3$ is given by

$$Y(C_4F_9OC(O)CH_3) = Y(C_4F_9OCHO(\bullet)CH_3)\left[\frac{\frac{k_{21}}{k_{19}}[O_2]}{\frac{k_{21}}{k_{19}}[O_2] + 1}\right] + C \quad \text{(II)}$$

The term "C" in expression II was added to account for the nonzero intercept in the *i*-$C_4F_9OC(O)CH_3$ yield plot and is discussed later. The curves in Figure 6 are fits of the above expressions to the experimental data. From the *i*-$C_4F_9OC(O)H$ data we derive $Y(i\text{-}C_4F_9OCHO(\bullet)CH_3) = 0.72 \pm 0.04$, $Y(C_4F_9OCH_2CH_2O(\bullet)) = 0.07 \pm 0.03$, and $k_{21}/k_{19} = 0.024 \pm 0.006$, while the *i*-$C_4F_9OC(O)CH_3$ data give $Y(i\text{-}C_4F_9OCHO(\bullet)CH_3) = 0.67 \pm 0.04$, $k_{21}/k_{19} = 0.028 \pm 0.008$ Torr^{-1}, and $C = 0.12 \pm 0.04$. It is gratifing to note that least-squares fits of expressions I and II to the variation of the yields of *i*-$C_4F_9OC(O)H$ and *i*-$C_4F_9OC(O)CH_3$ with $[O_2]$ give indistinguishable values of k_{21}/k_{19}. We choose to quote a final value of k_{21}/k_{19} which is an average of the two determinations with error limits that encompass the extremes of the individual determinations; $k_{21}/k_{19} = 0.026 \pm 0.010$ Torr^{-1}. In 1 atm of air at 296 K the O_2 partial pressure is 160 Torr and 81% of the *i*-$C_4F_9OCHO(\bullet)CH_3$ radicals will react with O_2 while the remainder will decompose via reaction 19. In the real atmosphere most of the oxidation of HFE-7200 will occur at elevated altitudes and hence temperatures and total pressures below that employed here. Lower temperature favors reaction 21 while lower total pressure (and hence O_2 partial pressure) favors reaction 19. Reaction 19 is a unimolecular decomposition reaction and will have a substantial activation barrier. As with other similar competitions (e.g., in the case of the $CF_3CFHO(\bullet)$ radical[4]), it is expected that the temperature effect will greatly dominate the pressure effect and that the atmospheric fate of *i*-$C_4F_9OCHO(\bullet)CH_3$ radicals is dominated by reaction with O_2.

At this point we need to return to the inclusion of the factor "C" in expression II. It is obvious from Figure 6 that the *i*-$C_4F_9OC(O)CH_3$ has a nonzero *y*-axis intercept. There are several possible causes of this intercept: (i) perhaps reaction 20 is important, (ii) perhaps there is a contribution due to a molecular channel of the peroxy radical self- and cross-reactions which gives the ester, or (iii) perhaps the ester is formed in the *i*-$C_4F_9OCHO_2(\bullet)CH_3 + HO_2$ reaction. The important conclusion from this study namely that the atmospheric fate of *i*-$C_4F_9OCHO(\bullet)CH_3$ radicals is dominated by reaction with O_2 is insensitive to the cause of the intercept.

As seen from Figure 6 the two observed products, *i*-$C_4F_9OC(O)H$ and *i*-$C_4F_9OC(O)CH_3$, account for close to 100% of the loss of HFE-7200. This result is quite remarkable considering the complexity of the chemical system. Two different peroxy radicals are formed, and these undergo self- and cross-reactions. The "molecular reaction channels" giving carbonyl and alcohol products which are important in nonfluorinated peroxy radical self-reactions[17] do not appear to be important for the peroxy radicals derived from HFE-7200. The evidence from the present work is that these self- and cross-reactions give predominately the corresponding alkoxy radicals. Finally, it is interesting to note that for experiments using hydrocarbons carried out in the absence of NO we usually observe the formation of hydroperoxides via the reaction $RO_2 + HO_2 \rightarrow ROOH + O_2$. The absence of hydroperoxides in the present work is similar to the behavior of the analogous compound $C_4F_9OCH_3$ (HFE-7100).[14] As with our previous study of HFE-7100, the absence of hydroperoxides can be rationalized several ways: (i) the $RO_2 + HO_2$ reaction is unusually slow, (ii) the $RO_2 + HO_2$ reaction does not give ROOH but instead produces the formate (the analogous $CH_3OCH_2O_2 + HO_2$ reaction gives a substantial formate yield[18]), (iii) ROOH is formed in the system but is consumed by secondary reaction with Cl atoms to regenerate the peroxy radical, or (iv) a combination of the above.

For completeness, a limited series of product experiments was performed in the presence of NO_x using mixtures of 6.5−7.1 mTorr of i-HFE-7200, 400 Torr of O_2, 100−420 mTorr of Cl_2, and 7−40 mTorr of NO in 700 Torr total pressure with N_2. When NO is present in the reaction mixtures, the alkoxy radicals are formed via reaction 3a rather than reaction 18. For experiments using the lowest NO concentrations the observed yields of *i*-$C_4F_9OC(O)H$ and *i*-$C_4F_9OC(O)CH_3$ were, within the experimental uncertainties, indistinguishable from those observed in the absence of NO. This shows that the fate of the alkoxy radicals is not dependent upon their source. For experiments using NO concentrations of 14 mTorr and higher the observed yields of both *i*-$C_4F_9OC(O)H$ and *i*-$C_4F_9OC(O)CH_3$ decreased with increasing [NO]. This behavior is ascribed to scavenging of the alkoxy radicals via reaction with NO_x to give nitrites and nitrates.

Implications for Atmospheric Chemistry. We present herein a substantial body of kinetic and mechanistic data pertaining to the atmospheric chemistry of HFE-7200. The atmospheric lifetime of HFE-7200 is determined by its reaction with OH radicals. The atmospheric lifetime of n-HFE-7200 is estimated to be 0.9 years while that of i-HFE-7200 is 0.7 years. Reaction with OH will give two different alkyl radicals; both will rapidly add O_2 and be converted into peroxy radicals which will in turn react with NO to give the corresponding alkoxy radicals, $C_4F_9OCHO(\bullet)CH_3$ and $C_4F_9OCH_2CH_2O(\bullet)$. We show here that the dominant atmospheric fate of $C_4F_9OCHO(\bullet)CH_3$ radicals is reaction with O_2 to give the ester $C_4F_9OC(O)CH_3$. In the present work we observe that the $C_4F_9OCH_2CH_2O(\bullet)$ radical is converted into the formate $C_4F_9OC(O)H$, but we are not able to establish the route by which this occurs. By analogy to the behavior of the $C_2H_5OCH_2CH_2O(\bullet)$ radical,[19] it seems likely that the atmospheric fate of $C_4F_9OCH_2CH_2O(\bullet)$ radical is decomposition via C−C bond scission (reaction 2).

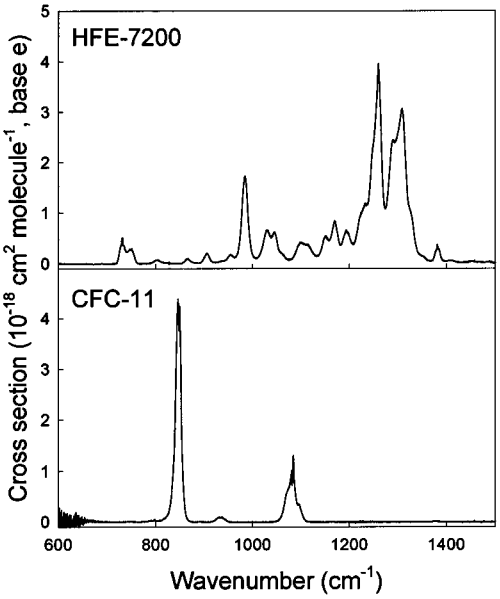

Figure 7. IR spectra of HFE-7200 (mixture of n- and i-isomers used commercially) and CFC-11.

In the present work we have used Cl atoms to initiate the oxidation of HFE-7200 whereas in the atmosphere initiation is provided by OH radical attack. There are no available data concerning the relative importance of attack of OH radicals on the $-CH_2-$ and $-CH_3$ groups in HFE-7200. In the present study we show that the majority of Cl atom reaction occurs at the $-CH_2-$ group. OH radicals are 39 times less reactive than Cl atoms toward HFE-7200, and it seems reasonable to suppose that OH radicals will be even more discriminating than Cl atoms. Hence, we conclude that the atmospheric oxidation will produce $C_4F_9OC(O)CH_3$ as the major and $C_4F_9OC(O)H$ as the minor product.

It is reported herein that the ester $C_4F_9OC(O)CH_3$ is rather unreactive toward Cl atoms and is likely to be similarly unreactive toward OH radicals. Organic compounds which react with Cl atoms with rate constants in the range $10^{-14}-10^{-13}$ cm^3 molecule^{-1} s^{-1} generally react faster with Cl atoms than with OH radicals.[9] Hence, we can use the value of $k(Cl + C_4F_9OC(O)CH_3) < 7 \times 10^{-13}$ cm^3 molecule^{-1} s^{-1} as an upper limit to $k(OH + C_4F_9OC(O)CH_3)$. Using a 24 h global average OH concentration of 7.5×10^5 cm^{-3}, we derive an estimated lower limit of 22 days for the atmospheric lifetime of $C_4F_9OC(O)CH_3$ with respect to reaction with OH radicals. In view of the polar nature of $C_4F_9OC(O)CH_3$ it is possible that the main atmospheric removal mechanism of this compound will be via wet/dry deposition and possibly photolysis. Unfortunately, there are no available data for the rates of these processes and hence it is not possible to provide an estimate of the atmospheric lifetime of $C_4F_9OC(O)CH_3$ at this time.

The atmospheric degradation of HFEs produce the same fluorinated radical species as formed during the degradation of HFCs. HFCs do not impact stratospheric ozone,[20] and the same conclusion applies to HFEs; HFE-7200 has an ozone depletion potential of zero. Finally we need to consider the potential for HFE-7200 to impact the radiative balance in the atmosphere. Using the method of Pinnock et al.[21] with the IR spectra shown in Figure 7, we calculate instantaneous radiative forcings for HFE-7200 and CFC-11 of 0.39 and 0.26 W/m^2, respectively. The global warming potential (GWP) of HFE-7200 can be estimated using the following expression:

$$\mathrm{GWP} = \frac{\mathrm{IF}_{\mathrm{HFE-7200}}}{\mathrm{IF}_{\mathrm{CFC-11}}} \frac{\tau_{\mathrm{HFE-7200}}}{\tau_{\mathrm{CFC-11}}} \frac{M_{\mathrm{CFC-11}}}{M_{\mathrm{HFE-7200}}} \frac{1 - \exp\left(-\frac{t}{\tau_{\mathrm{HFE-7200}}}\right)}{1 - \exp\left(-\frac{t}{\tau_{\mathrm{CFC-11}}}\right)}$$

Here IF, τ, and M are the radiative forcing, lifetime, and molecular weight of the two compounds and t is the time horizon over which the forcing is integrated. CFC-11 has an atmospheric lifetime of approximately 50 years.[21] Commercial HFE-7200 samples are mixtures of 35% n-HFE-7200 and 65% i-HFE-7200. To evaluate the GWP of such samples it is appropriate to use an atmospheric lifetime of 0.77 years, which is a weighted average of the two different isomers. For 20 and 100 year time horizons the GWPs of HFE-7200 are estimated to be 0.036 and 0.014, respectively. The GWP of HFE-7200 is approximately 30−120 times less than that of typical CFCs such as CFC-11, CFC-12, and CFC-113.

Acknowledgment. We thank Fred Behr (3M Corp.) for supplying samples of HFE-7200, Robert Meagher and Mark McIntosh for their help in conducting experiments at Ford, Roscoe Carter (Ford) for his expertise in analysis of the IR spectra, Mike Hurley (Ford) for supplying the IR spectra shown in Figure 7, and Steve Japar (Ford) for helpful discussions. The work at Risø was supported by the European Union, and the work at MIT was supported by 3M.

References and Notes

(1) Molina, M. J.; Rowland, F. S. *Nature* **1974**, *249*, 810.
(2) Farman, J. D.; Gardiner, B. G.; Shanklin, J. D. *Nature* **1985**, *315*, 207.
(3) Product information sheet from 3M Specialty Chemicals Division, 1996.
(4) Wallington, T. J.; Schneider, W. F.; Worsnop, D. R.; Nielsen, O. J.; Sehested J.; Debruyn, W. J.; Shorter, J. A. *Environ. Sci. Technol.* **1994**, *28*, 320.
(5) Tang, Y. **1993**. Atmospheric Fate of Various Fluorocarbons. MS Thesis, Massachusetts Institute of Technology.
(6) Hansen, K. B.; Wilbrandt, R.; Pagsberg, P. *Rev. Sci. Instrum.* **1979**, *50*, 1532.
(7) Wallington, T. J.; Japar, S. M. *J. Atmos. Chem.* **1989**, *9*, 399.
(8) Bilde, M.; Møgelberg, T. E.; Sehested, J.; Nielsen, O. J.; Wallington, T. J.; Hurley, M. D.; Japar, S. M.; Dill, M.; Orkin, V. L.; Buckley, T. J.; Huie, R. E.; Kurylo, M. J. *J. Phys. Chem. A* **1997**, *101*, 3514.
(9) DeMore W. B.; Sander S. P.; Golden, D. M.; Hampson, R. F.; Kurylo, M. J.; Howard, C. J.; Ravishankara, A. R.; Kolb, C. E.; Molina, M. J. *JPL Publication No. 97-4*; NASA Jet Propulsion Lab.: Pasadena, CA, 1997.
(10) Prinn R. G.; Weiss R. F.; Miller B. R.; Huang, J.; Alyea, F. N.; Cunnold, D. M.; Fraser, P. J.; Hartley, D. E.; Simmonds, P. G. *Science* **1995**, *269*, 187.
(11) Wallington, T. J.; Ellermann, T.; Nielsen, O. J. *Res. Chem. Intermed.* **1994**, *20*, 265−276.
(12) Wallington, T. J.; Hurley, M. D.; Maricq, M. M.; Sehested, J.; Nielsen, O. J.; Ellermann, T. *Int. J. Chem. Kinet.* **1993**, *25*, 651.
(13) Wallington, T. J.; Hurley, M. D. *Chem. Phys. Lett.* **1992**, *189*, 437.
(14) Wallington, T. J.; Schneider, W. F.; Sehested, J.; Bilde, M.; Platz, J.; Nielsen, O. J.; Christensen, L. K.; Molina, M. J.; Molina, L. T.; Wooldridge, P. *J. Phys. Chem. A* **1997**, *101*, 8264.
(15) Mallard, W. G.; Westley, F.; Heron, J. T.; Hampson, R. F. *NIST Chemical Kinetics Database*, version 6.0; NIST: Gaithersburg, MD, 1994.
(16) Wallington, T. J.; Guschin, A.; Stein, T. N. N.; Platz, J.; Sehested, J.; Christensen, L. K.; Nielsen O. J. *J. Phys. Chem. A* **1998**, *102*, 1152.
(17) Wallington, T. J.; Dagaut, P.; Kurylo, M. J. *Chem. Rev.* **1992**, *92*, 667.
(18) Wallington, T. J.; Hurley, M. D.; Ball, J. C.; Jenkin, M. E. *Chem. Phys. Lett.* **1993**, *211*, 41.
(19) Wallington, T. J.; Japar, S. M. *Environ. Sci. Technol.* **1991**, *25*, 410.
(20) Wallington, T. J.; Schneider, W. F.; Sehested, J.; Nielsen, O. J. *J. Chem. Soc., Faraday Discuss.* **1995**, *100*, 55.
(21) Pinnock, S.; Hurley, M. D.; Shine, K. P.; Wallington, T. J.; Smyth, T. J. *J. Geophys. Res.* **1995**, *100*, 23227.